A Homotopy Surface Cutting using Paths Crossing in Geodesic Distance

Anuwat Dechvijankit[1], Hiroshi Nagahashi[2] and Kota Aoki[2]
[1]*Department of Computational Intelligence and Systems Science, Tokyo Institute of Technology, Yokohama, Japan*
[2]*Imaging Science and Engineering Laboratory, Tokyo Institute of Technology, Yokohama, Japan*

Keywords: Geodesic Distance, Graph Cut, Homotopy, Surface Parameterization, Topology.

Abstract: Topology is a property of surfaces that plays a major role in computer graphics. Processing or analysis between two surfaces generally requires both of them to be in same topology. There are many tools or applications such as parameterization or remeshing that require disk topology surfaces as input. Therefore, it is important to convert any surfaces to be same as a topological disk. The common procedure is to define a graph of edges inside the surface that should be split into two edges and to turn the surface into topological disk. We call it as homotopy cutting. Problems become more difficult when dealing with high genus surfaces such as a torus. Based on a novel method, we present an enhancement method to generate a cut graph in high-genus surface for homotopy cutting. By using geodesic properties of each edge, we can generate equally or more suitable edge-graph than original method while keeping similar performance and stability as original one.

1 INTRODUCTION

Geometry processing is an important research in 3D computer graphics field. Without efficient algorithms, it is very difficult to develop any kinds of advanced applications for end-users. Some of important applications in 3D computer graphics, such as texture mapping (Bennis et al., 1991), normal mapping (Cohen et al., 1998), remeshing (Hormann and Greiner, 2000) and parameterization (Tutte, 1963; Floater, 1997) require a specific topology of input mesh. There are many cases where topological disk surface is specified for further processing. Such topological requirement in input mesh has significant impact on several researches. There are many properties in each mesh such as closed/open, holes and genus which require different approach on them.

When processing a mesh that requires disk topology input, all kinds of meshes have different measures. An open surface has originally the same topology as a disk which can pass directly, but may need to be taken care in case of containing holes. Some problems arise when dealing with a closed surface since it has different topology from the disk. The process of surface cutting into a disk is required. In case of sphere topology, it does not require much processes; only short graph edge is necessary. However, there need some processes to ensure the quality of graph edges in homotopy cutting. The problem becomes more complex and more interesting when dealing with high genus surfaces.

This paper presents a homotopy cutting on high genus surfaces. Our approach is an enhancement of a novel method (Gu et al., 2002) in homotopy cutting; cutting surfaces into disks. A benefit of this method is to be able to handle any kinds of 2-manifold surfaces, regardless of specific topology. We present an algorithm that creates a cut graph on the area where geodesic path comes from different directions in exact geodesic distance (Mitchell et al., 1987; Surazhsky et al., 2005) (see example in figure 1). With some extra calculation, we can define equally or more appropriate cut graph from original method while keeping performance and stability.

Figure 1: Geodesic distance radius from a starting point on genus 1 rocket arm model. At the hole (tunnel), we can see some sharp pattern which can be recognize as geodesic path came from different directions.

Dechvijankit A., Nagahashi H. and Aoki K..
A Homotopy Surface Cutting using Paths Crossing in Geodesic Distance.
DOI: 10.5220/0005302601300137
In *Proceedings of the 10th International Conference on Computer Graphics Theory and Applications* (GRAPP-2015), pages 130-137
ISBN: 978-989-758-087-1

Notations

Before explaining various algorithms of homotopy, let us define basic notations. We represent a 2-manifold triangular surface or mesh by $\mathscr{M} := (V,F)$, where $V := \{v_i \in \mathbb{R}^3 \mid i = 1,...,n_v\}$ is a set of n_v vertices and $F := \{f_i(a,b,c) \mid i = 1,...,n_f : a,b,c = 1,...,n_v : a \neq b \neq c\}$ is a set of n_f faces. We also define $E := \{e_i(a,b) \mid i = 1,...,n_e : a,b = 1,...,n_v : a \neq b\}$ as a set of n_e edges found in the surface $\mathscr{M}$. We assume that the mesh has genus g topology.

2 RELATED WORKS

As for a topic of topological converting in the past years, there was a novel work by (Erickson and Har-Peled, 2002) that studied the problem of cutting a topological surface into a disk efficiently. They proposed a cutting method that gave some elegant theoretical guarantees. However, the algorithm is very complex to be implemented. It finds the shortest loop path connecting vertices to the vertex itself by using a front propagation technique, and then tests if the considering loop path reduces the surface genus or simply cuts the surface into two pieces. It has topologically-sufficient cut as $2g$ loops. The generation of minimal length cut that converts a high genus surface into a topological disk is a NP-hard problem. One method is a brute force approach which consumes a lot of time. However, it is an approximation of the shortest cut graph calculated in $O(g^2 n \log n)$ where n denotes complexity of the surface. (Erickson and Whittlesey, 2005) studied about a greedy homotopy basis and improved its calculation speed in $O(n \log n)$ by using a straightforward application of Dijkstra's shortest path algorithm (Dijkstra, 1959).

From the efficiency point of view, it is important to compute non-trivial cycles on orientable surfaces. Non-trivial cycles mean non-contractible and non-separating cycles which guarantee the topological surface cutting into disk. Recently, (Kutz, 2006) presents an algorithm that computes a shortest non-trivial cycle in $O(n \log n)$ on an orientable combinatorial surface of bounded genus. The algorithm is based on universal-cover constructions to find short cycles.

There are several studies that try to define a cut graph by surface properties. A study by (Patanè et al., 2007) presents an algorithm that builds up the cut graph on the iso-contours from Reeb graph which codes the topology of a given surface $\mathscr{M}$ in a combinatorial structure and generates loops together. There are deep studies by (Dey et al., 2008; Dey et al., 2013) that show how to recognize short handle and tunnel loops in a surface by using Reeb graph. Another study by (Jin et al., 2013) presents an algorithm to compute the shortest homotopic loop with negative Euler characteristic based on the surface hyperbolic uniformization metric. They also demonstrated two applications: constructing extremal quasi-conformal mappings between same topology surfaces, and detecting homotopy between two paths or cycles on a surface.

There is an iterative method called "geometry images" by (Gu et al., 2002), which is similar to that of (Dey, 1994). This method presents a remeshing approach using square surface parameterization to create a mapping between irregular surface $\mathscr{M}$ in $\mathbb{R}^3$ domain, and square plane in $\mathbb{R}^2$ domain. To get low error on the remeshing, they present how to create a cut graph from any kinds of surfaces $\mathscr{M}$ regardless from the pre-analysis of topology and boundary edges.

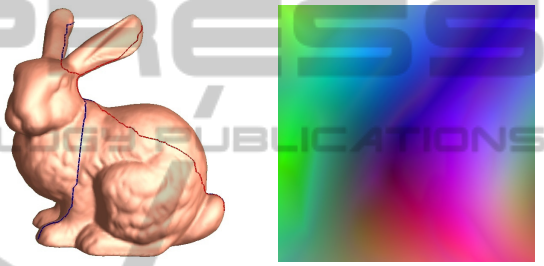

(a) Geometry of surface (b) Geometry image

Figure 2: A geometry image.

Since our approach is based on (Gu et al., 2002) approach, we explain in section 3 how it creates a cut graph for homotopy cutting on an irregular surface $\mathscr{M}$ with genus g.

3 PREVIOUS ALGORITHM

The algorithm of (Gu et al., 2002) is divided into two parts, i.e., homotopy cutting and its augmentation. The augmentation aims to improve its subsequent square planar domain parameterization. We explain the first part that involves the definition of a cut graph and a converting surface $\mathscr{M}$ into disk.

At the beginning, when the mesh $\mathscr{M}$ has boundaries, let $\mathscr{B}$ be the set of original boundary edges that remain unchanged in the whole process and will be included in final cut graph ρ. It first starts by removing a single seed triangle from the mesh. At this moment, each edge of the seed triangle is adjacent to only one triangle respectively (see figure 3(b)). After removing the seed triangle from the mesh, there are two processing phases.

In the first phase, it repeatedly detects an edge adjacent exactly to one triangle that is not in $\mathscr{B}$, and

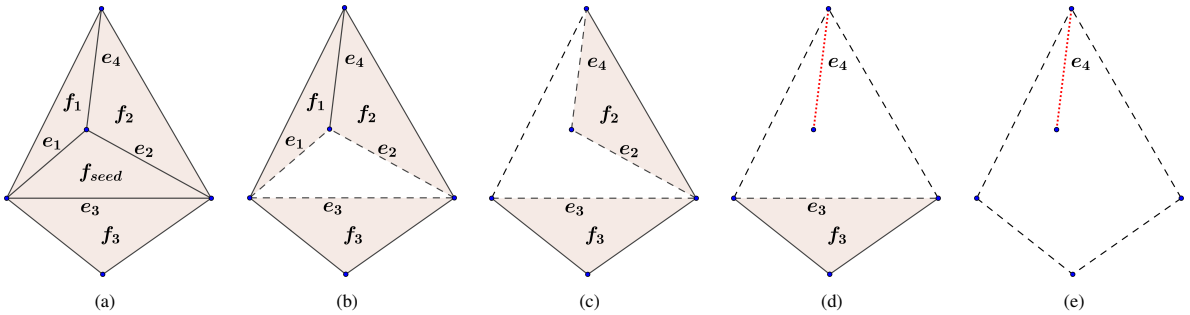

Figure 3: Processes from removing a seed triangle from a mesh. Dash lines mean edges that are adjacent to only one triangle at the moment. (a) shows before removing stage. (b) shows after removing the seed triangle; that is, edges e_1,e_2 and e_3 are adjacent to only one triangle. Assume that geodesic distance from f_{seed} to e_1 is the smallest. (c) shows the result of removing edge e_1 and face f_1. The edge e_4 become the one that adjacent to only one triangle. Let e_2 is next smallest geodesic distance. (d) shows the result of removing e_2 and f_2. The edge e_4 becomes a candidate of cut graph edge (red dot line). (e) shows the result of next step that removing e_3 and f_3.

removes both the edge and the triangle from the mesh structure. The rest two edges are left (see figure 3(c)). If the rest edges of the removing triangle are not adjacent to any triangle, then the edges will become one of candidates of cut graph (see figure 3(d)). Generally, removing one edge and one triangle triggers additional two edges to be adjacent to only one triangle further. Because of the above condition, the removing propagation will keep spreading out from the seed triangle according to geodesic distance in order to get minimum radius result. Since a 2-manifold triangle mesh is being processed, every triangle will be removed eventually. Therefore, this phase ends when there is no triangle left and there remain only edges and their vertices as candidate cut graph edges. At this point, the cut ρ consists of a set of connecting $2g$ loops.

In the second phase, we again iteratively detect a valence-1 vertex and its corresponding edge, and remove both the vertex and the edge (see figure 4). The purpose of this phase is to remove unnecessary dangling edges remained in the first phase. The dangling edges will be repeatedly trimmed away until there is no valence-1 vertex left in the cut ρ. There are only edges that form connected loops as a cut graph in the cut ρ. At last, all loops in ρ are straightened by computing a local shortest path in each loop. Finally, the connected $2g$ loop cut graph in ρ is homotopy basis: a cut graph that converts the surface into a topological disk patch.

For the case of closed surface of genus $g = 0$, the overall processes from this part will generate the cut ρ that consists of only one vertex. To enable the mapping into planar domain, we add two adjacent edges of the vertex into the cut graph ρ. On the other hand, for the case of a mesh having one or more holes, it will result in connected graphs between any holes' edges and homotopy basis.

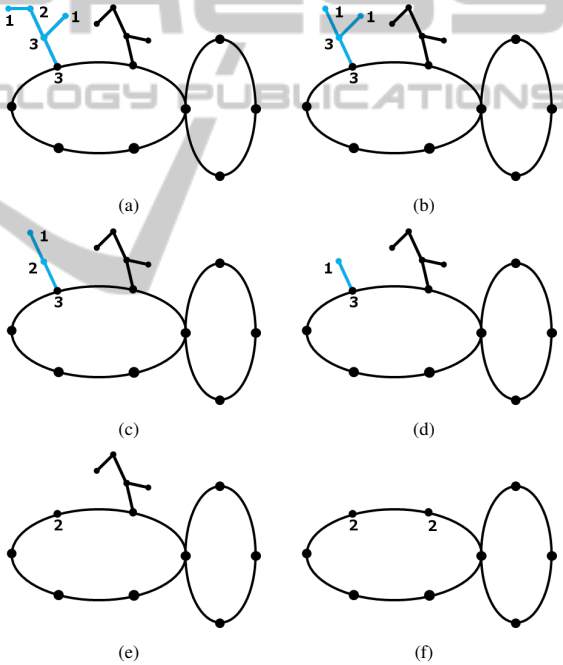

Figure 4: Process on removing dangling edges. The numbers on vertices indicate present valence number. We focus on the removing of blue dangling edges. (a) shows initial state where there are two valence-1 edges. (b) - (d) show the following steps that remove valence-1 edge along with its vertex. (e) shows that all blue dangling edges have been removed. (f) shows the process of removing other dangling edges until valence-1 edge has not been found in graph.

4 GEODESIC DISTANCE

The algorithm by (Gu et al., 2002) creates front propagation on geodesic distance. We consider an exact

geodesic distance proposed by (Mitchell et al., 1987) as knows as MMP algorithm. It computes exact shortest paths on a triangular mesh. These paths typically cut across faces in the mesh, which is different from typical Dijkstra shortest paths (Dijkstra, 1959) that run across edges in the mesh.

MMP algorithm creates a geodesic path for "single source and all destinations" scheme. The algorithm computes a set of intervals of each edge. An interval represents an accessible pencil of lines from its pseudo-source. Each interval also acts as a pseudo-source to propagate across faces of the rest of mesh. The algorithm propagates the distance information out from the source in a Dijkstra-like fashion which can traceback any positions on mesh to the source. Figure 5 shows the concept of propagation of the algorithm where intervals i_β and i_γ can be traceback to v_{source} through i_α.

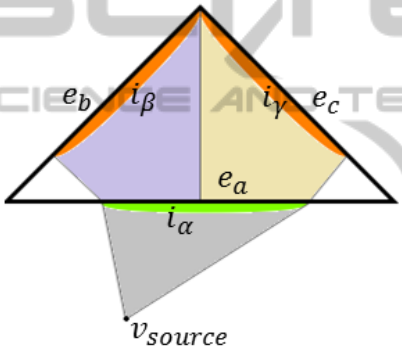

Figure 5: Propagation scheme of MMP algorithm: interval i_α on edge e_a propagates distance pencil paths across an adjacent face to adjacent edges e_b and e_c.

The performance of MMP algorithm : they prove a worst case running time of $O(n^2 \log n)$ when n is the number of mesh edges. However in practical calculation, it can achieve on 100K triangles mesh within a few seconds. Also, there is an approximate version of MMP algorithm proposed by (Surazhsky et al., 2005) that can speed up the calculation by trying to merge an interval with adjacent intervals on the same edge before starting the propagation.

Notations

After calculating the exact geodesic distance from a vertex v_s, each edge e_i that is not a boundary one, has a set of m intervals $I_{e_i} := \{i_{e_{i,j}}(f_p, e_p, D) \mid i = 1,...,n_v, j = 1,...,m\}$, where f_p represents the face where propagation of interval's pseudo-source across and e_p represents the edge that has interval's pseudo-source. D represents another information about geodesic distance of considering interval.

5 OUR APPROACH

Given a triangular 2-manifold mesh $\mathscr{M}$ without any topological information about genus g, we adopt a geometry image method (Gu et al., 2002) to define $2g$ cut loop graph for homotopy basis. Instead of having a cut graph along the propagation by geodesic distance criteria, we try to have a cut graph in the area where it has the same geodesic distance but its pseudo-sources come from different edges and faces.

To define such area, we calculate the exact geodesic distance from a source vertex v_s by MMP algorithm (Mitchell et al., 1987) and then analyze the set of intervals in each edge e_i. First, we define edges whose intervals have pseudo-sources laid on both side of adjacent faces. However, this case typically can detect few edges and cannot cover all areas where the cut graph should exist. Second, we define remaining edges whose intervals cannot be a pseudo-source of adjacent edges. We define these two specific characteristic edges as a set of edges $\tilde{E}$. At this point, $\tilde{E}$ contains a lot of unnecessary dangling edges. Therefore, we eliminate them from $\tilde{E}$ by the same approach in the original method.

We ensure that the cut graph has non-separating cycles by considering neighbor edges of $\tilde{E}$. We define a set of neighbor edges as $\hat{E}$, then the candidate cut graph edges can be given by $\rho \equiv (\tilde{E} \cup \hat{E})$, and the rest edges $\acute{E}$ are given as $\acute{E} \equiv (E - \rho)$. However, ρ may contain contractible cycles too. Therefore, we again need to define non-separating and non-contractible cycles from ρ. We follow similar basis from the original method by removing an edge exactly adjacent to one triangle. However, we create priority of removing edges in a queue according to $\acute{E}$, $\hat{E}$ and $\tilde{E}$. From this point, we follow the remaining original processes: removing dangling edges and shorten loop.

We explain in details how to define the set $\tilde{E}$ and how to ensure the generation of non-separating and non-contractible cut graph.

5.1 Pseudo-sources of Intervals from Both Sides

The main idea of our approach is to detect areas where geodesic distance's paths are crossing together, like wave occlusion. Since we generate a cut graph, we define such areas as a set of edges.

First, we detect an edge e_i whose intervals I_{e_i} satisfy the condition: if there is an interval that f_p is not same as other intervals then we consider $e_i \in \tilde{E}$. From figure 6(a), we can see clearly that e_a has two intervals $i_{e_{a,1}}$ and $i_{e_{a,2}}$, where first one has a pseudo-source

from f_l while second one has another pseudo-source from f_r. Typically, this kind of edges can be found a few in mesh (green edges in figure 7(a)).

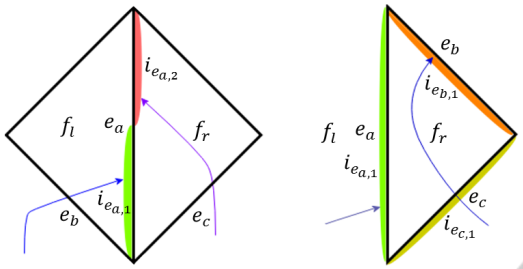

(a) from both sides type (b) non-propagation type

Figure 6: Two types of edges that are considered as area of crossing geodesic distance's path.

5.2 Non-propagation Edge Intervals

Along with the edge type described in section 5.1, we need to define another edge type in cut graph. That is, this type of edges are nearby crossing of geodesic distance's paths.

We detect an edge e_i whose intervals I_{e_i} satisfy the condition: all intervals have pseudo-sources from same face f_p (pseudo-source edge e_p can be different). Let opposite face be $f_{\bar{p}}$ and other two adjacent edges of $f_{\bar{p}}$ be $e_{\bar{i}_1}$ and $e_{\bar{i}_2}$. We consider both $e_{\bar{i}_1}$ and $e_{\bar{i}_2}$ edges by the following conditions.

- Edge intervals have pseudo-sources from both sides (section 5.1).
- Edge intervals have $e_p \neq e_i$.

If both $e_{\bar{i}_1}$ and $e_{\bar{i}_2}$ match one of above conditions, then we consider $e_i \in \tilde{E}$.

Considering an edge e_a in figure 6(b), we can clearly see that edges e_b and e_c of opposite face f_r ($e_{\bar{i}_1}$ and $e_{\bar{i}_2}$) have all intervals where their pseudo-sources are not on e_a, so we include e_a into $\tilde{E}$. Vise-versa, when we are considering edge e_c; we can clearly see that edge e_b has an interval where its pseudo-source is on e_c so we exclude e_c from $\tilde{E}$.

Typically, this kind of edges can be found a lot in mesh and cover all areas of mesh (blue edges in figure 7(a)). Therefore, we need to eliminate unnecessary edges in $\tilde{E}$. Present state of cut graph looks similar to dangling edges in original one so we run the same iterative process to remove the valance-1 vertices in the graph.

5.3 Ensure for Non-separating Cycles

After detecting the edges in $\tilde{E}$ whose geodesic distance's paths are crossing, we aim to create a homotopy cut graph which requires non-separating and non-contractible cycles from $\tilde{E}$.

At this stage, $\tilde{E}$ may typically contains separating or contractible cycles (see figure 7(b)). For separating cycles issue, we define all edges in $\hat{E}$ to be neighbors of each edge in $\tilde{E}$. We consider that a set of edges $\rho \equiv (\tilde{E} \cup \hat{E})$ contains $2g$ loops inside it.

5.4 Prioritize Removing-edge Queues

After making sure that ρ contains $2g$ loops, we try to create a valid cut graph along them. From this condition, we must eliminate edges that cause contractible cycles from ρ and maintain non-separating property. Also, there are non-considered edges $\acute{E} \equiv (E - \rho)$ which will be excluded from the cut graph.

One advantage of the original method is to guarantee a valid cut graph when the propagation finished. Because of that, we used the original propagation scheme. However, we also want the cut graph to be around $\tilde{E}$ as first priority and around $\hat{E}$ as second priority. Therefore, we altered the orders of removing edge in the original propagation scheme. We created three removing-edge queues rather than single queue in the original one. Each queue contains edges based on: $\acute{E}$, $\hat{E}$ and $\tilde{E}$. And we mark each of them for low-to-high priority in the order of $\acute{E}$, $\hat{E}$ and $\tilde{E}$.

First, we remove faces around v_s as seed triangles. Next, we iteratively analyze edges (adjacent only one triangle) in a non-empty queue under the conditions that the edge and its adjacent face on low priority queue are removed first and the edge with shortest geodesic distance in the queue will be removed first.

After the propagation terminates and all queues become empty, the remaining edges contain $2g$ loops with non-separating and non-contractible properties. Again, we might shorten each loop for better quality in some further applications. At last, we generate a cut graph that enables to convert the mesh with genus g into topological disk patch.

6 EXPERIMENTAL RESULTS

We tested the algorithms on a workstation PC (Intel Xeon^{TM}10 cores running at 2.50GHz) by using parameterization results from both original (Gu et al., 2002) and our approach methods. We also recorded time consumed for generating cut graphs. We manually selected a vertex in the input mesh as v_s then generated a cut graph. To create cut graphs from both methods with similar conditions, we want the both propagations to be spread out from a same location.

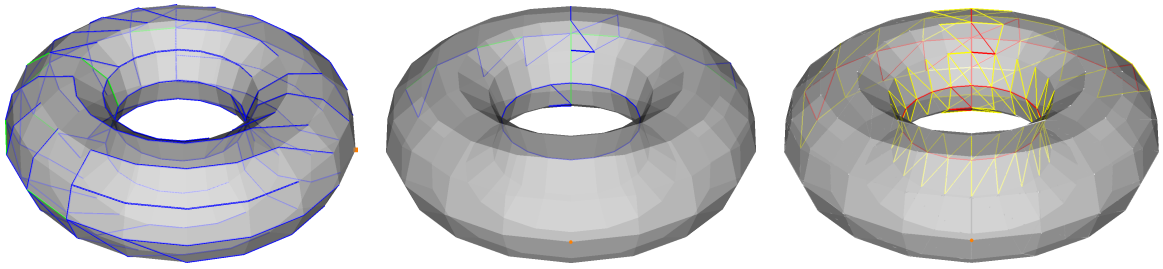

(a) (b) (c)

Figure 7: Processes to define $\tilde{E}$ and $\hat{E}$ on a torus model. (a) shows green colored edges that their intervals' pseudo-sources are from both sides, and blue colored edges that their intervals have not propagated. (b) shows the graph after removing dangling edges. (c) shows $\tilde{E}$ in red color and $\hat{E}$ in yellow color.

Although the original algorithm removes single seed triangle, our approach removes seed triangles around v_s. Therefore, we altered how to remove a seed triangle in original one to be same as our approach. With this alternation, it should not affect to overall performance in original one. Also, we applied shorten loops process after the propagation terminated.

After converting the input mesh into disk topological patch, we applied stretch-minimizing parameterization by (Yoshizawa et al., 2004). We evaluated the parameterization results from both methods by using L^2 error (the root-mean-square stretch over all direction in planar domain) proposed by (Sander et al., 2001; Sander et al., 2002). See more details in appendix.

After evaluating several meshes whose genuses are greater than or equal 1 ($g \geq 1$), we noticed that original method and our approach can generate very similar or same cut graphs on asymmetry lookalike meshes in most cases. However, on some symmetrical shapes, cut graphs can be different from each others. Therefore, we selected some results which have noticeable difference on cut graphs between original and our approaches, and do parameterizations.

As shown in table 1, our approach can deliver lower L^2 error than the original one in most cases. There are some cases that the original one has a large error value while our approach can deliver a small error. Although, our approach might double calculation time but it can deliver results very fast even on high-details meshes. Also, we did the experiment using single-thread runtime which can be speeded up by parallel computation when defining edges $\tilde{E}$.

We show some visual results obtained from our experiments in figure 8. Note that all meshes do not contain any holes and case 02-03, 04-05, 06-07 and 08-09 are same models with different v_s location.

Table 1: Experimental results. Blue and green cells indicate lower errors in comparison.

case	genus	time (sec)		square		circular	
		original	our	original	our	original	our
01	1	0.006	0.009	1.351	1.335	1.493	1.446
02	1	0.014	0.030	1.492	1.468	1.687	1.663
03	1	0.014	0.029	1.562	1.636	1.800	2.102
04	1	0.040	0.106	1.551	1.417	2.011	1.635
05	1	0.040	0.106	1.561	1.362	1.924	1.538
06	2	0.028	0.051	1.667	1.466	2.246	1.701
07	2	0.028	0.052	1.390	1.442	1.603	1.554
08	3	0.489	1.217	1.457	1.452	1.688	1.679
09	3	0.527	1.228	2.041	2.025	9.279	9.827
10	3	0.263	0.574	471.2	1.509	4.068	1.978
11	3	0.497	1.163	939.2	1.625	6.348	4.115
12	3	0.110	0.142	221.3K	79.9K	383.2K	203.4K

7 CONCLUSIONS

We presented an enhancement method to generate a cut graph in high-genus surface for homotopy cutting. Cut graph is generated based on an exact geodesic distance theory, by detecting areas where geodesic distance's paths are crossing together. We showed how to detect these areas into a set of edges by analyzing edges' intervals. Then, we also showed how to ensure non-separating and non-contractible cycles by including neighbor edges into the set and applying original approach with minor adjustments in propagation queues. We can generate equally or more suitable edge-graph than the original method while keeping similar performance and stability as original one.

An open topic of this propagation scheme is, it still requires manual starting location of propagation (seed triangle or v_s in our approach). The quality of cut graph depends on user specific positions. To generate an optimal cut graph on a high genus surface, it is better to have shortest cut loop where it passes through on each surface's tunnel. Therefore, it is interesting to consider how to define starting location v_s for generating optimal cut graph.

ACKNOWLEDGEMENTS

The images in figures 2 are from (Gu et al., 2002) paper and presentation file. Models are courtesy of the AIM@SHAPE repository. Special thanks are given to Danil Kirsanov for exact geodesic distance code, to Shin Yoshizawa for parameterization code and to the anonymous reviewers for comments and suggestions. This study is supported by JSPS KAKENHI (Grant Number 24300035).

REFERENCES

Bennis, C., Vézien, J.-M., and Iglésias, G. (1991). Piecewise surface flattening for non-distorted texture mapping. *SIGGRAPH Comput. Graph.*, 25(4):237–246.

Cohen, J., Olano, M., and Manocha, D. (1998). Appearance-preserving simplification. In *Proceedings of the 25th Annual Conference on Computer Graphics and Interactive Techniques*, SIGGRAPH '98, pages 115–122, New York, NY, USA. ACM.

Dey, T. K. (1994). A new technique to compute polygonal schema for 2-manifolds with application to null-homotopy detection. In *Proceedings of the Tenth Annual Symposium on Computational Geometry*, SCG '94, pages 277–284, New York, NY, USA. ACM.

Dey, T. K., Fan, F., and Wang, Y. (2013). An efficient computation of handle and tunnel loops via reeb graphs. *ACM Trans. Graph.*, 32(4):32:1–32:10.

Dey, T. K., Li, K., Sun, J., and Cohen-Steiner, D. (2008). Computing geometry-aware handle and tunnel loops in 3d models. *ACM Trans. Graph.*, 27(3):45:1–45:9.

Dijkstra, E. W. (1959). A note on two problems in connexion with graphs. *NUMERISCHE MATHEMATIK*, 1(1):269–271.

Erickson, J. and Har-Peled, S. (2002). Optimally cutting a surface into a disk. In *Proceedings of the eighteenth annual symposium on Computational geometry*, SCG '02, pages 244–253, New York, NY, USA. ACM.

Erickson, J. and Whittlesey, K. (2005). Greedy optimal homotopy and homology generators. In *Proceedings of the Sixteenth Annual ACM-SIAM Symposium on Discrete Algorithms*, SODA '05, pages 1038–1046, Philadelphia, PA, USA. Society for Industrial and Applied Mathematics.

Floater, M. S. (1997). Parametrization and smooth approximation of surface triangulations. *Comput. Aided Geom. Des.*, 14:231–250.

Gu, X., Gortler, S. J., and Hoppe, H. (2002). Geometry images. *ACM Trans. Graph.*, 21(3):355–361.

Hormann, K. and Greiner, G. (2000). Quadrilateral remeshing. In *Proceedings of Vision, Modeling and Vizualization, 2000*, pages 153–162.

Jin, M., Ding, N., and Yang, Y. (2013). Computing shortest homotopic cycles on polyhedral surfaces with hyperbolic uniformization metric. *Comput. Aided Des.*, 45(2):113–123.

Kutz, M. (2006). Computing shortest non-trivial cycles on orientable surfaces of bounded genus in almost linear time. In *Proceedings of the Twenty-second Annual Symposium on Computational Geometry*, SCG '06, pages 430–438, New York, NY, USA. ACM.

Mitchell, J. S. B., Mount, D. M., and Papadimitriou, C. H. (1987). The discrete geodesic problem. *SIAM J. Comput.*, 16(4):647–668.

Patanè, G., Spagnuolo, M., and Falcidieno, B. (2007). Families of cut-graphs for bordered meshes with arbitrary genus. *Graph. Models*, 69(2):119–138.

Sander, P. V., Gortler, S. J., Snyder, J., and Hoppe, H. (2002). Signal-specialized parametrization. In *Proceedings of the 13th Eurographics Workshop on Rendering*, EGRW '02, pages 87–98, Aire-la-Ville, Switzerland, Switzerland. Eurographics Association.

Sander, P. V., Snyder, J., Gortler, S. J., and Hoppe, H. (2001). Texture mapping progressive meshes. In *Proceedings of the 28th Annual Conference on Computer Graphics and Interactive Techniques*, SIGGRAPH '01, pages 409–416, New York, NY, USA. ACM.

Surazhsky, V., Surazhsky, T., Kirsanov, D., Gortler, S. J., and Hoppe, H. (2005). Fast exact and approximate geodesics on meshes. *ACM Trans. Graph.*, 24(3):553–560.

Tutte, W. T. (1963). How to draw a graph. *Proceedings of The London Mathematical Society*, s3-13:743–767.

Yoshizawa, S., Belyaev, A., and Seidel, H.-P. (2004). A fast and simple stretch-minimizing mesh parameterization. In *SMI '04: Proceedings of the Shape Modeling International 2004*, pages 200–208, Washington, DC, USA. IEEE Computer Society.

APPENDIX

Given a triangle T with 2D planar coordinates p_1, p_2, p_3 where $p_i = (s_i, t_i)$ and corresponding 3D coordinates q_1, q_2, q_3. Since the mapping is affine, its partial derivatives are constant over s and t directions and given by:

$$S_s = \partial S/\partial s = (q_1(t_2 - t_3) + q_2(t_3 - t_1) + q_3(t_1 - t_2))/2A_P$$
$$S_t = \partial S/\partial t = (q_1(t_2 - t_3) + q_2(t_3 - t_1) + q_3(t_1 - t_2))/2A_P$$

where A_P denotes area of triangle (p_1, p_2, p_3) in planar domain.

Let denote $\Gamma(T)$ and $\gamma(T)$ are maximum and minimum lengths eigenvalues of Jacobian $[S_s, S_t]$, represent the largest and smallest length obtained when mapping unit vectors from planar domain to the surface. The local stretch norms over a triangle T is given by:

$$L^2(T) = \sqrt{(\Gamma^2 + \gamma^2)/2} = \sqrt{(S_s^2 + S_t^2)/2}$$

We define norms over the entire mesh $\mathscr{M} = \{T_i\}$:

$$L^2(\mathscr{M}) = \sqrt{\sum_{T_i \in \mathscr{M}} (L^2(T_i)^2 A_{T_i}) / \sum_{T_i \in \mathscr{M}} A_{T_i}}$$

where A_{T_i} denotes area of triangle T_i in 3D domain.

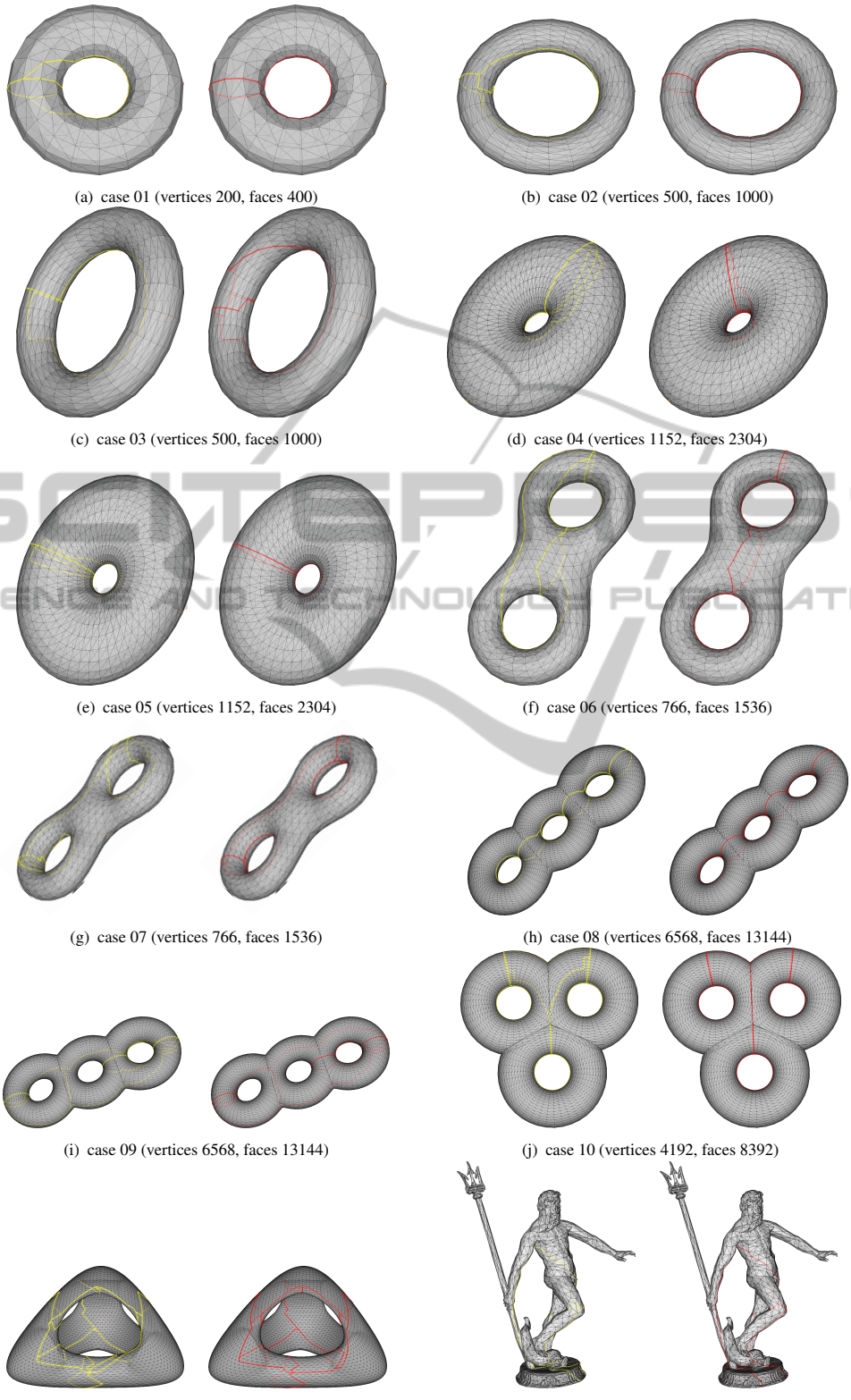

(a) case 01 (vertices 200, faces 400)

(b) case 02 (vertices 500, faces 1000)

(c) case 03 (vertices 500, faces 1000)

(d) case 04 (vertices 1152, faces 2304)

(e) case 05 (vertices 1152, faces 2304)

(f) case 06 (vertices 766, faces 1536)

(g) case 07 (vertices 766, faces 1536)

(h) case 08 (vertices 6568, faces 13144)

(i) case 09 (vertices 6568, faces 13144)

(j) case 10 (vertices 4192, faces 8392)

(k) case 11 (vertices 6652, faces 13312)

(l) case 12 (vertices 2496, faces 5000)

Figure 8: Results of homotopy cutting from original (Gu et al., 2002) and our approach methods. The meshes having yellow line are results obtained by original approach. The meshes having red line are our results.